Chiral Stationary Phases Based on Aleuritic Acid as Chiral Spacer Arms: Middle and Terminal Chiral Factors *vs.* Chromatographic Separation Performance

Kun Li,[a] Xiaoxue Wang,[a] Shujie Xing,[b] Baoshan Tang,[c] Wenwen Zhang,[a,*] Qingsong Zhu,[a] and Kunfeng Liu [a]

The enantiomeric monomer of aleuritic acid was used as a spacer arm to prepare chiral stationary phases (CSP1~3) for chiral selectors containing only aleuritic acid, S-phenylglycinol (S-PGL), and R,R-diphenylethylene-diamine (*R,R*-DPEDA). The Fourier transform infrared (FTIR), thermo-gravimetry (TG), elemental analysis, and solid state nuclear magnetic resonance (SSNMR) characterizations showed that the three stationary phases were coupled depending on the route design, and the grafting ratio was 12.4%, 78.2%, and 32.7%, respectively. The first specimen CSP1, containing only aleuritic acid, was able to separate 4 of the 9 target compounds. Separation of 6 compounds was achieved by the introduction of the single chiral factor *S*-PGL's (CSP2). After introduction of the double chiral factor *R,R*-DPEDA (CSP3), separation of 8 compounds was achieved. Although the grafting ratio of *R,R*-DPEDA in CSP3 was only 32.7%, and the increase in carbon content was only 3.08% compared with that of CSP1, which was less than half of that of CSP2. Thus, CSP3 showed significantly higher separation selectivity. The difference in chiral factors led to the reverse resolution order of enantiomers under certain conditions for some compounds. The chiral spacer arm was shown to be important in separation and in the preparation methods of novel structural CSPs.

DOI: 10.15376/biores.21.4.10108-10126

Keywords: Enantiomers; Brush-type CSPs; Vicinal diol; Chiral selector; Grafting yield

Contact information: a: Xinyang Agriculture and Forestry University, Xinyang, 464000, China; b: Luohe Vocational Technology College, Luohe, 462000, China; c: Institute of Highland Forest Science, Chinese Academy of Forestry, Yunnan Kunming 650233, China;
** Corresponding author: zhangwenwen1105@163.com; (W.W. Zhang)*

INTRODUCTION

As human demand for optically pure monomers continues to grow, the awareness of chiral separation has been gradually increasing (Qian *et al.* 2023). Chiral chromatography has become an important way to obtain enantiomers due to its high efficiency, rapidity, convenience, and high reproducibility (Francotte 2001). The chiral stationary phase in the chromatography column is one of the core separation factors of chiral chromatography (Liu *et al.* 2023; Wang *et al.* 2024). In order to obtain chiral stationary phase materials with wider adaptability, higher selectivity, and separation efficiency, chiral stationary phase materials with different structural characteristics and separation performances have been widely explored, which has become a research hotspot in this field (Scriba 2012; Teixeira *et al.* 2019; Zhang *et al.* 2022). Chiral stationary phase material is mainly composed of a support substance, a spacer arm, and a chiral selector

(Felletti *et al.* 2023; Papp *et al.* 2024). Due to its good chemical stability, reactivity, and structural strength, silica gel is widely used in chromatography and chiral chromatography stationary phase substance (Bui *et al.* 2023; Nawrocki 1997; Sobańska 2021). In the preparation of chiral stationary phase materials of various structural chiral selectors, especially in the preparation of "brush type" (Pirkle type), amino and its derivatives, peptides, cyclodextrin, cellulose, polysaccharide, chiral natural products, and pharmaceuticals as stationary phase materials for chiral selectors, this approach has achieved many research advances and promoted the development of preparation and separation theory for chiral stationary phase materials (Wang *et al.* 2021; Aboul-Enein *et al.* 2022; Gonçalves *et al.* 2022; He *et al.* 2022; Ohji *et al.* 2022; Ma *et al.* 2023).

During the preparation of the chiral stationary phase, the spacer arm is the bridge between the chiral selector and the support substance (Pirkle and Murray 1993; Zhang *et al.* 2021). At present, there is no consensus regarding the role of the spacer arm in chiral recognition. Some scholars believe that the spacer arm of different lengths has a significant effect on chiral recognition due to the channeling of the spacer arm (Berthod *et al.* 1993; Ho Hyun and Hun Kim 2004; Thunberg *et al.* 2004). Studies have also shown that the length of the spacer arm does not lead to a significant difference in the separation performance of the chiral stationary phase (Lai and Ng 2003). In literature reports available, chiral stationary phases (CSPs) have been prepared by achiral substances as the spacer arms (Bargmann-Leyder *et al.* 1994; Thunberg *et al.* 2004). To the best of the authors' knowledge, there have been no studies of preparation of CSPs based on chiral substances as spacer arms. The preparation of chiral stationary phase materials by using chiral substance as space arms is of great significance for further study of the role of spacer arms in chiral separation processes and the exploration of chiral stationary phase separation materials with special structures.

Aleuritic acid is a renewable and chiral polyhydroxy fatty acid derived from natural shellac resin, namely 9.10,16-trihydroxyhexadecanoic acid, and the molecule is $C_{16}H_{32}O_5$ (Ali *et al.* 2024; Benítez *et al.* 2015; Benítez *et al.* 2016). The development and utilization of aleuritic acid in many applications has been widely explored by previous researchers (Ali *et al.* 2022; Li Kun 2019b). For example, Gaikar proposed a mathematical model for the hydrolysis of seedlac and a purification method of aleuritic acid by Indion 850 polymer resin (Nagappayya and Gaikar 2010). Gupta fabricated novel aleuritic tryptophan and tried to synthesize (*in situ*) silver nanoparticles and utilized as high efficiency dye synthesized solar cell (Gupta *et al.* 2018). Given that the 9,10-site consists of chiral carbons, theoretically, aleuritic acid has two sets of enantiomers in the threo and erythro configurations (Ames 1968). However, previous studies have found that the extracted natural aleuritic acid contains only one enantiomer of the threo configuration (Li Kun 2019a). By supercritical fluid chromatography, the optical isomer monomer of aleuritic acid of threo configuration was successfully prepared, providing raw materials for the research and utilization of the separation materials for chiral characteristics of aleuritic acid as the core.

Given that both ends of the molecular chain contain active sites, such as hydroxyl groups and carboxyl groups, the aleuritic acid can be easily bonded to the support substances of silica gel. As a vicinal diol type chiral moiety, the 9,10-site chiral hydroxyl group in the chain not only provides an active site for introducing other functional groups, but it also possibly enhances chiral recognition ability as a chiral factor. Therefore, this study explored the preparation method of this novel stationary phase material with chiral spacer arm with aleuritic acid as the main starting material. The effects of introduction of

chiral selectors were investigated with different structure types at the end of the molecular chain on separation performance. This study lays a foundation for further investigation of the separating effect of spacer arm in chiral stationary phase, and preparation method of chiral stationary phase with special structure.

EXPERIMENTAL

Materials

3-(Triethoxysilyl)propyl isocyanate (TPI, purity≥95%, GC), 4-dimethylamino-pyridine (DMAP, purity≥99%, titration), (1R,2R)-(+)-1,2-diphenylethylenediamine (DPEDA, purity≥98%, GC), and (S)-(+)-2-phenylglycinol (PGL, purity≥98%, GC) were purchased from Tokyo Chemical Industry Co. Ltd. (Shanghai, China). 3,5-Dinitrobenzoyl chloride (DNBC) (purity≥99%, GC), N-hydroxysuccinimide (NHS) (purity≥98%, GC), and 1-(3-dimethylaminopropyl)-3-ethylcarbodiimide hydrochloride (purity≥98%, GC) were purchased from Aladdin Co. Ltd. (Shanghai, China). (±)-1-Phenylethanol (purity≥97%, GC), DL-mandelic acid (purity≥99%, GC), (±)-2-chloromandelic acid (purity≥98%, GC), (±)-benzoin (purity≥99.5%, GC), (±)-1-(4-chlorophenyl)-3-buten-1-ol (purity≥97%), (±)-1,1′-Bi(2-naphthol) (purity≥99%, GC), DL-phenylalanine (purity ≥98%, HPLC), (±)-baclofen (purity≥98%, T), (±)-naringenin (purity≥98%, HPLC), (±)-Amlodipine (purity≥98%, HPLC) all were purchased from Sigma-Aldrich Co. Ltd. (Shanghai, China). Porous spherical silica (SG, 10 μm) was purchased from Sepax Technologies Co. Ltd. (Suzhou, China).

Methods

Preparation and determination of aleuritic acid enantiomers

Preparation of aleuritic acid enantiomer was carried out by supercritical fluid chromatography (SFC). CHIRALPAK AY-H (3.0 cm I.D. ×25 cm×5 μm) column, carbon dioxide and alcohol volume ratio 70:30 of mobile phase, 70 mL/min speed, 35°C column temperature, 208 nm detection wavelength, 7.78 mg/mL injection concentration, 3 mL injection volume every time.

Chiral determination of aleuritic acid was done by high performance liquid chromatography and evaporative light-scattering detector (HPLC-ELSD). The use of an ELSD was dictated by the absence of relevant chromophores in the aleuretic acid structure. The column used was a DAICEL CHIRAL PAK IF (25 cm × 0.46 cm i.d., 5 μm), with 0.5 mL/min flow rate of mobile phase, 0.1% formic acid solution (40%): acetonitrile (60%) of mobile phase composition, 30 °C column temperature. The parameter setting of ELSD detector was evaporator temperature 70 °C, drift tube was kept at 60 °C, and carrier gas (high purity nitrogen) rate was set at 1.6 L/min. The results show that aleuritic acid was an enantiomer of threo configuration and the content of two enantiomers were 65.5% and 34.5%, respectively. Therefore, the enantiomeric excess (*ee*%) value of aleuritic acid was 31%.

Enantiomers of aleuritic acid prepared by SFC were as follows. ^{1}H-NMR (500 MHz, DMSO) $\delta\times10^{-6}$: 11.97 (s, 1H, H-1), 4.32 (s, 1H, H-16), 4.14 (s, 2H, HOH-9, 10), 3.35 (t, J=5.96, 2H, H-16), 3.18 (s, 2H, H-9, 10), 2.17 (t, J=7.2, 2H, H-2), 1.10~1.47(m, 22H, H-3,4,5,6,7,8,11,12,13,14,15). ^{13}C-NMR (126 MHz, DMSO) $\delta\times10^{-6}$: 174.55 (C-1), 73.16 (C-9, C-10), 60.77 (C-16), 33.70 (C-2), 32.59 (C-8, C-11), 32.26, 29.21, 29.16, 28.87, 28.61, 25.89, 25.71, 25.61, 24.55 (C-3,4,5,6,7,12,13,14,15).

Preparation of CSPs based on aleuritic acid

The synthesis route of CSPs based on aleuritic acid is presented in scheme 1. The 16-hydroxy of aleuritic acid was used as the active site to react with isocyanate group of TPI. Then the CSPs were obtained by stepwise coupled reaction. The whole point is that CSP1 contained only 9,10-chiral carbon of aleuritic acid as chiral factors. Then, chiral selectors with single (CSP2) and double (CSP3) chiral centre were introduced by amidation with the terminal carboxyl of aleuritic acid.

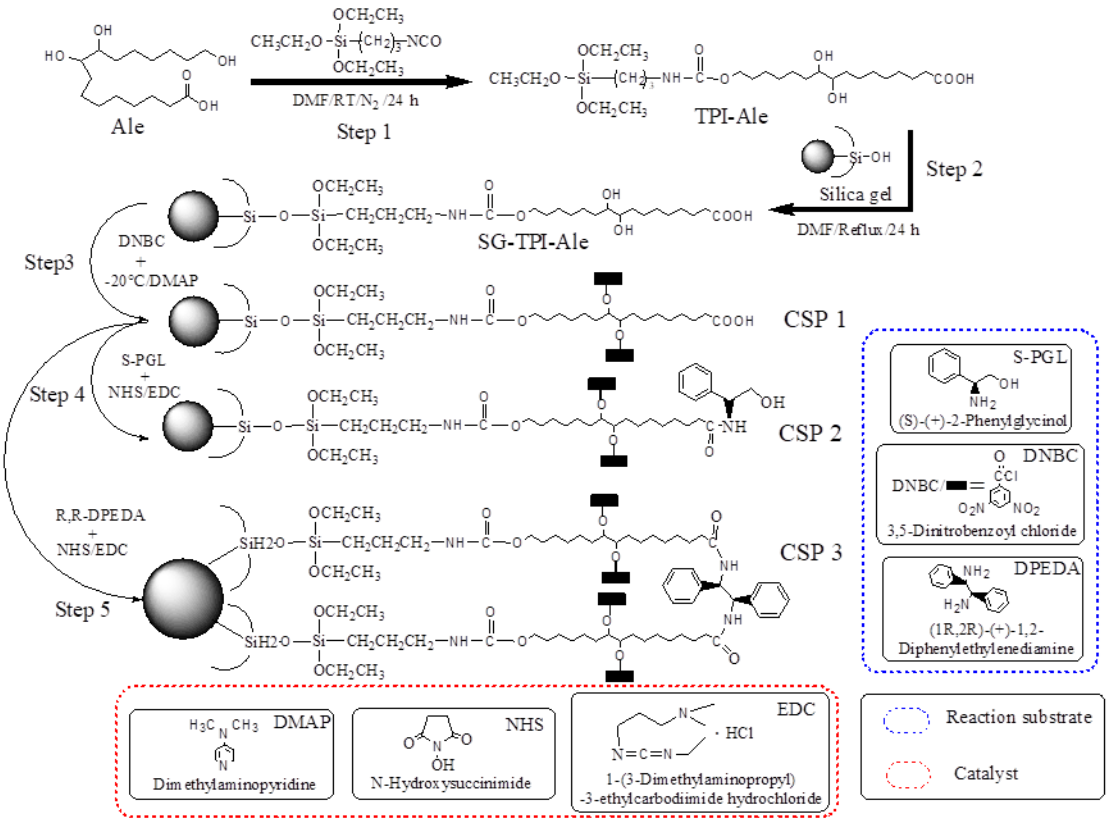

Scheme 1. Schematic diagram of synthesis route of CSPs based on aleuritic acid

Synthesis method of CSP1

1.20 g (3.94 mmol) of aleuritic acid (Ale) and 0.975 g (3.94 mmol) of isocyanic acid 3-(triethoxysilyl) propyl ester (TPI) were dissolved in 25 mL of previously dried N,N-dimethylformamide (DMF) solution, and the reaction was performed at room temperature for 24 h under stirring. After cooling, 4.0 g of spherical silica gel (SG) that had been activated and dried beforehand was added, and 10 mL of anhydrous DMF was added. After refluxing for 24 h, it was washed with 90% ethanol, methanol, deionized water, methanol, respectively, and dried at 80 °C under vacuum, and SG-TPI-Ale was obtained. The product obtained above was placed in a 100 mL round-bottom flask, and 40 mL of anhydrous DMF was added. 3.635 g (15.76 mmol, 4 eq of hydroxy in aleuritic acid) of 3,5-dinitrobenzoyl chloride (DNBC) was taken and dissolved in 10 mL of anhydrous DMF, and 36.35 mg DMAP (1% Wt, DNBC) was added; under the condition of -20 °C, the nitrogen protection reaction was conducted for 24 h, and it washed with DMF, methanol, deionized water, and methanol, respectively, and then dried under vacuum at 80 °C to obtain CSP1.

Synthesis method of CSP2

0.6 g of the above CSP1 sample and 0.358 g (1.87 mmol) of 1-(3-dimethylamino-propyl)-3-ethylcarbodiimide hydrochloride (EDC) were placed in 30 mL of anhydrous DMF. After reaction for 20 min, 0.179 g (1.55 mmol) of N-hydroxysuccinimide (NHS) was added; the reaction continued for 20 min, and 0.321 g (2.34 mmol) of (*S*)-(+)-phenylglycinol (PGL) was added; under the condition of -20 °C, the nitrogen protection reaction was conducted for 24 h, and it was washed with DMF, methanol, deionized water, and methanol, respectively, and then dried under vacuum at 80 ° C to obtain CSP2.

Synthesis method of CSP3

0.6 g of the above CSP1 sample and 0.358 g (1.87 mmol) of EDC were placed in 30 mL of 90% ethanol solution. After reaction for 20 min, 0.179 g (1.55 mmol) of NHS was added; the reaction continued for 20 min, and 0.182 g (0.857 mmol) (*1R,2R*)-(+)-1,2-diphenylethylenediamine (DPEDA) was added; under the condition of -20 °C, the nitrogen protection reaction was conducted for 24 h, and it washed with 90% alcohol, methanol, deionized water, and methanol, respectively, and then dried under vacuum at 80 °C to obtain CSP3.

Characterization of CSPs

Attenuated Total Reflectance-Fourier Transform Infrared Spectroscopy (ATR-FTIR): Samples were analyzed using an ATR-FTIR spectrometer (Tensor-27, Bruker, Germany) equipped with an ATR accessory. Spectral data were acquired in the wavenumber range of 4000 to 400 cm^{-1} with a resolution of 4 cm^{-1} and 32 accumulated scans.

Differential Scanning Calorimetry (DSC) Analysis: Accurately weighed samples were analyzed using a differential scanning calorimeter (DSC 200 F3, Netzsch, Germany). Measurements were conducted in the temperature range of 0 to 400°C at a heating rate of 10°C/min under a high-purity nitrogen atmosphere (purity≥99.99%). Aluminum crucibles were employed, with liquid nitrogen as the cooling medium. Purge and protective gas flow rates were maintained at 80 mL/min and 50 mL/min, respectively.

Thermogravimetric (TG) Analysis: The prepared samples were analyzed using a thermogravimetric analyzer (STA 2500, Netzsch, Germany). Measurements were performed in the temperature range of 30 to 800°C at a heating rate of 10 °C/min, with a sample mass of 5 to 8 mg. Alumina ceramic crucibles were employed, utilizing liquid nitrogen as the cooling medium under a high-purity nitrogen atmosphere (purity≥99.99%). Purge and protective gas flow rates were maintained at 100 and 80 mL/min, respectively.

Elemental Analysis: Accurately weighed samples (TPI-Ale, SG-TPI-Ale, CSP1, CSP2, CSP3) were tightly encapsulated in tin foil and loaded into the autosampler. Analyses were performed using an elemental analyzer (Flash 2000, Thermo Fisher Scientific, USA) with the following parameters: 2 s injection time, 20 min run time per sample, combustion chamber temperature of 900°C, hydrogen flow rate of 140 mL/min, and carrier gas flow rate of 140 mL/min. The calibration standard employed was bis(tert-butyl) benzothiophene (BBOT; molecular formula: $C_{26}H_{26}N_2O_2S$).

Nuclear Magnetic Resonance (NMR): The reaction product of 3-(triethoxysilyl) propyl isocyanate with aleuritic acid (TPI-Ale) was analyzed in deuterated dimethyl sulfoxide (DMSO-d6) with tetramethylsilane (TMS) as the internal standard.

Solid-State NMR (SSNMR): Experiments were performed on an AVANCE III wide-bore solid-state NMR spectrometer (Bruker, Germany) using a 3.2 mm dual-

resonance high-resolution MAS probe. Acquisition parameters included: 5 kHz sample spinning ratio, 2 ms cross-polarization contact time, and 1500 accumulated scans.

Calculation of grafting ratio: The formula for calculating the grafting ratio based on the change of carbon content was as follows:

$$G_Y = \frac{C_A}{C_T} \times 100\% \quad (1)$$

In formula 1, G_Y represents the grafting ratio /%, C_A is the actual measured increased percentage of carbon content /%, and C_T represents the theoretical increased percentage of carbon content in the sample /%.

Chromatographic column packing method: A column with dimensions of 4.6 mm I.D. × 150 mm was selected. The stationary phase consisted of 10 μm spherical silica particles whose surface had been modified through the aforementioned method. The packing slurry was prepared using methanol/isopropanol (90:10, v/v) and packed under 40 MPa pressure. After column preparation, sequential washing procedures were performed with methanol, isopropanol, methanol, water, and methanol (30 min each solvent) until chromatographic baseline stabilization was achieved. Chiral resolution experiments were initiated following confirmation of stable baseline performance.

RESULTS AND DISCUSSION

Preparation of CSPs with Aleuritic Acid as Chiral Spacer Arm

Structural characterization of TPI-Ale

The reaction product of isocyanic acid 3-(triethoxysilyl) propyl ester (TPI) and aleuritic acid (Ale) was marked as TPI-Ale. As shown in Fig. 1, the molecular weight per unit of charge of the product TPI-Ale was 551 *m*/z.

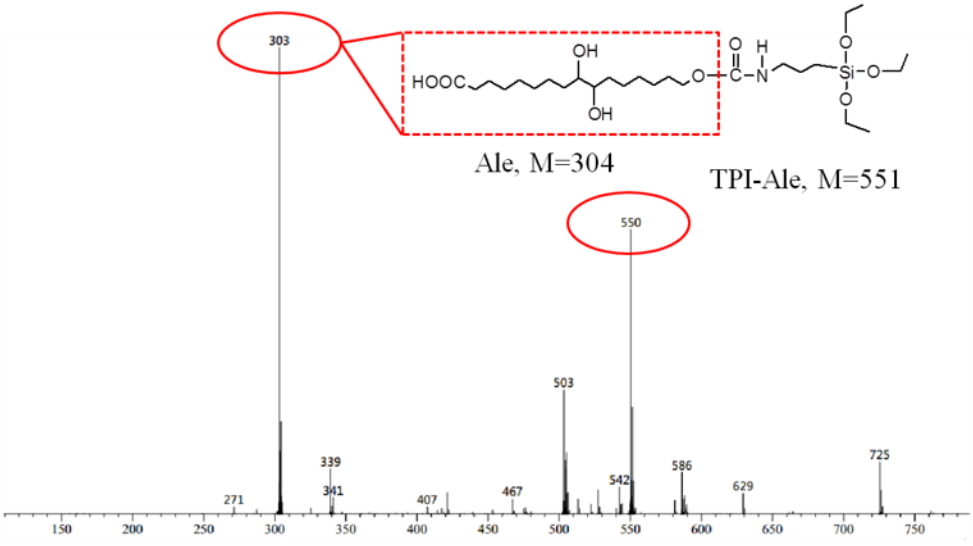

Fig. 1. ESI source mass spectrometry of TPI-Ale

In the negative ion mode of ESI source mass spectrometry, the base peak of molecular weight of 550 *m*/*z* in the product indicated a crosslinking reaction between the isocyanate group and the hydroxyl group of the aleuritic acid. In the nuclear magnetic carbon spectrum (Fig. 2), TPI-Ale showed an absorbance peak of carbonyl carbon in the -

NH-COO-acylamino structure at δ162.50, which corresponded to the results of mass spectrometry in Fig. 1, indicating a reaction between isocyanate groups and the hydroxyl group of aleuritic acid. In addition, in the TPI-Ale product, the absorbance peak of C-16 site hydroxyl carbon of δ60.77 aleuritic acid almost disappeared, indicating that the isocyanate group reacted with the C-16 site hydroxyl group of δ60.77 aleuritic acid.

As compared with silica gel, the characteristic absorbance peak of the amidation-modified chiral stationary phase at 3400 cm^{-1} was red-shifted (Fig. 3). Based on previous studies, the chiral CSP after red-shifting generally had better separating effect than before (Zhang *et al.* 2014). The wavenumbers 2845 cm^{-1} and 2920 cm^{-1} correspond to the stretching vibration absorbance peaks of C-H bond of alkyl carbon chain, and as the reaction proceeds, CSP2 and CSP3 show obvious blue-shifting.

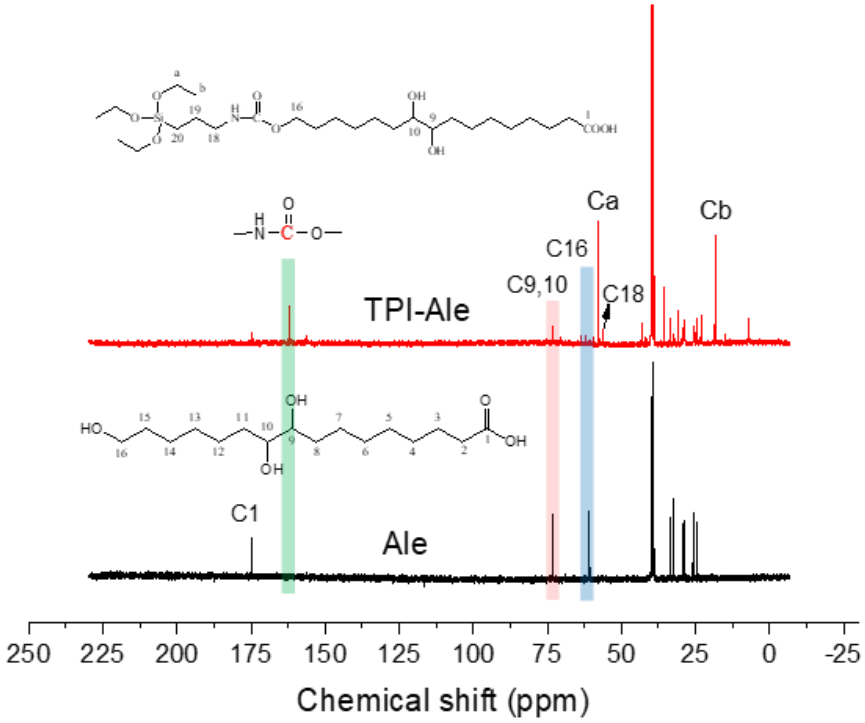

Fig. 2. ^{13}C-NMR of Ale and TPI-Ale

Structural characterization of CSPs with aleuritic acid as chiral spacer arm

CSP2 and CSP3 exhibited new characteristic absorbance peaks around 2954 cm^{-1}, which are the results of mutual superposition of absorbance peaks between the =C-H bond on the aromatic group of phenylglycinol (PGL) and diphenylethylenediamine (DPEDA) and the C-H bond on the alkyl carbon chain. Due to the hydrogen bonding, the C=O absorbance peak of the aleuritic acid optical monomer was red shifted to 1690 cm^{-1}. From the TPI-Ale, the C=O bond absorbance peak produced a distinct separation tendency, such that the 1705 cm^{-1} absorbance peak of the ester bond C=O, and amide bond C=O absorbance peak were near 1662 cm^{-1}.

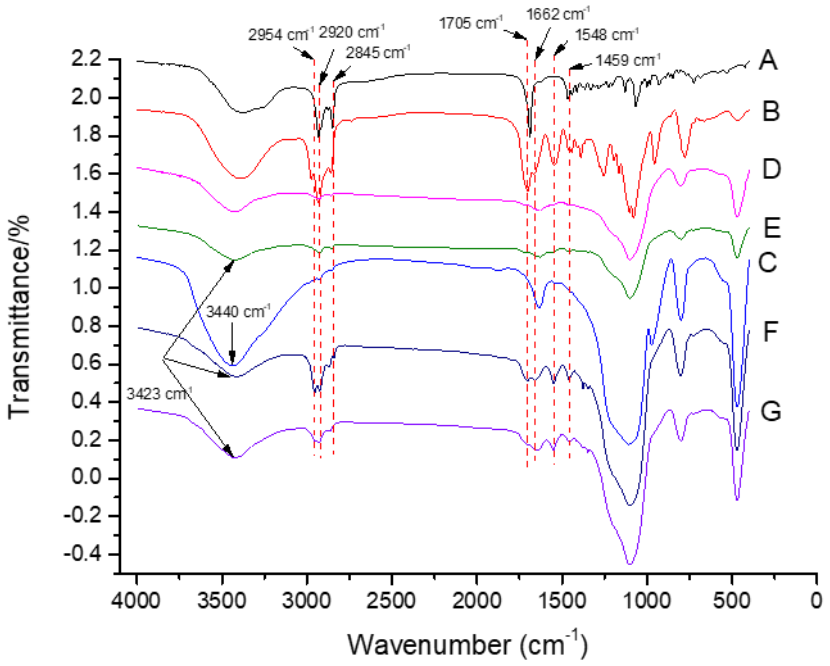

A)Ale, B) TPI-Ale, C) Silica gel, D) SG-TPI-Ale, E) CSP1, F) CSP2, G) CSP3

Fig. 3. FTIR of CSPs for aleuritic acid as chiral arm

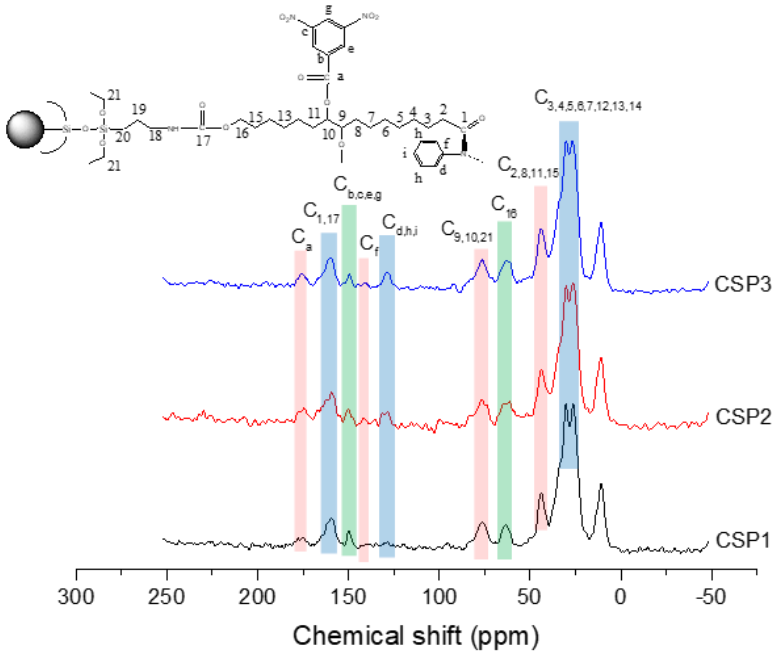

Fig. 4. SSNMR spectrum of CSPs for aleuritic acid as chiral arm

For CSP2 and CSP3, due to introduction of terminal amino group, amide bond C=O absorbance peak near 1662 cm^{-1}, the deformation vibration absorbance peak of N-H at 1548 cm^{-1}, and the stretching vibration absorbance peak of the C=C bond of the aromatic group at 1459 cm^{-1} were significantly enhanced, indicating the success of the derivative reaction of terminal amidation.

The solid-state nuclear magnetic ^{13}C spectrum could further confirm (Fig. 4) the structural changes of CSP2 and CSP3 obtained after CSP1 and terminal-derived chiral selectors of different structure types. Compared with CSP1, CSP2 and CSP3 had distinct separation tendency at the absorbance peak belonging to ester group C=O carbon at δ175.8 and amide group C=O carbon at δ159.8 CSP2, especially CSP2 with higher grafting ratio of *S*-PGL, which were structural characteristics of the terminal carboxyl group of aleuritic acid in CSP1 reacting with different structures of arylamine to form a novel amide. δ150.3 was the aryl carbon peak belonging to the 3,5-dinitrobenzoyl group. CSP2 and CSP3 had unsubstituted aromatic carbon peaks belonging to *S*-PGL and *R,R*-DPEDA at δ141.6 and δ128.8, further indicating the two organic amine monomers reacted with the grafted carboxyl group in CSP1.

Thermogravimetric Analysis of CSPs based on Aleuritic Acid as Chiral Spacer Arm

The weight loss percentage in the thermogravimetric curve of aleuritic acid group CSP material can reflect the changing process of organic matter content on the surface of silica gel to some extent, and from the grafting of aleuritic acid to the surface of silica gel (sample C to F in Fig. 5), its thermal weight loss percentage was shown in Table 1.

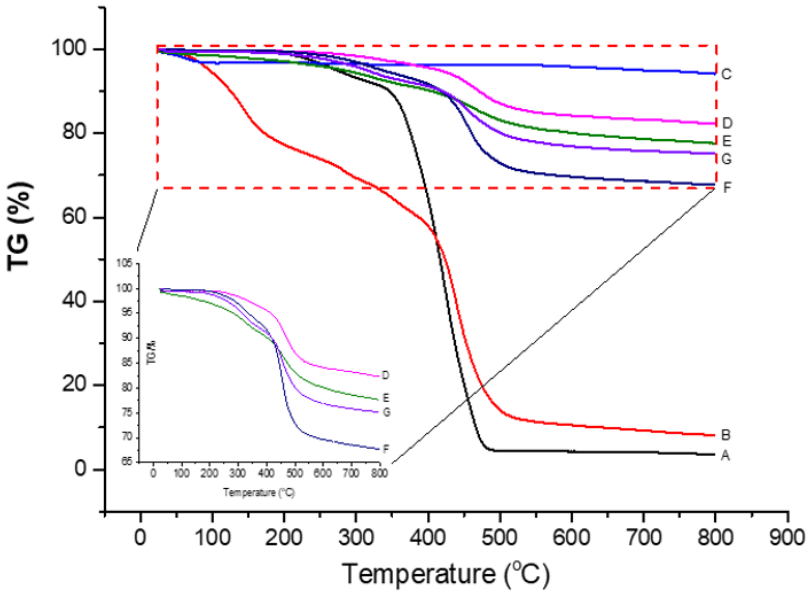

A) Ale, B) TPI-Ale, C SG-TPI-Ale, D) CSP1, E) CSP2, F) CSP3

Fig. 5. TG curves variation of CSPs for aleuritic acid as chiral arm

After deducting the ratio of thermal weight loss of bare silica gel, the approximate grafting ratio of the three aleuritic acid group CSPs were changed significantly. Compared with SG-TPI-Ale, the thermal weight loss percentage of CSP1 was increased by 4.69% after derivatization with DNBC. With CSP1 as the starting material, the weight loss percentage shown by the thermogravimetric curve of CSP2 and CSP3 was increased by 9.89% and 3.4%, respectively. The structural features of substituents in CSPs, particularly aromatic moieties, exert a significant influence on the chiral separation performance of the materials(Li *et al.* 2023; Shi *et al.* 2020; Shi *et al.* 2022). Based on the change in weight loss percentage, the increase of thermal weight loss percentage represented the proceeding

of the grafting reaction and the occurrence of the derivative reaction. The weight loss percentage of CSP2 after *S*-PGL was derived at the end of aleuritic acid, and grafting ratio of *R,R*-DPEDA was lower than that of *S*-PGL due to the steric hindrance of diamine. However, it was clear that the weight loss percentage in the thermogravimetric curve alone cannot accurately reflect the change in the grafting ratio of each derivatization step during the preparation.

Elemental analysis results of the product are shown in Fig. 6. The figure shows that the silica gel did not contain the N element, and the contents of C and H elements were extremely low. As the grafting reaction proceeded, the elemental content of the reaction product increased steadily. Among them, taking the carbon content as an example, the C content reached 12.6% in CSP1, 20.3% in CSP2, and 15.7% in CSP3. The increase of carbon content on silica gel indicated the occurrence of grafting reaction. The sum of the contents of N, C, and H elements in CSP1, CSP2 and CSP3 was 16.7%, 25.8%, and 20.4%, respectively, which was relatively in keeping with the weight loss percentage in the TG curves of the three CSP samples, suggesting the reaction substrate was grafted to the surface of the silica gel according to the experimental design route.

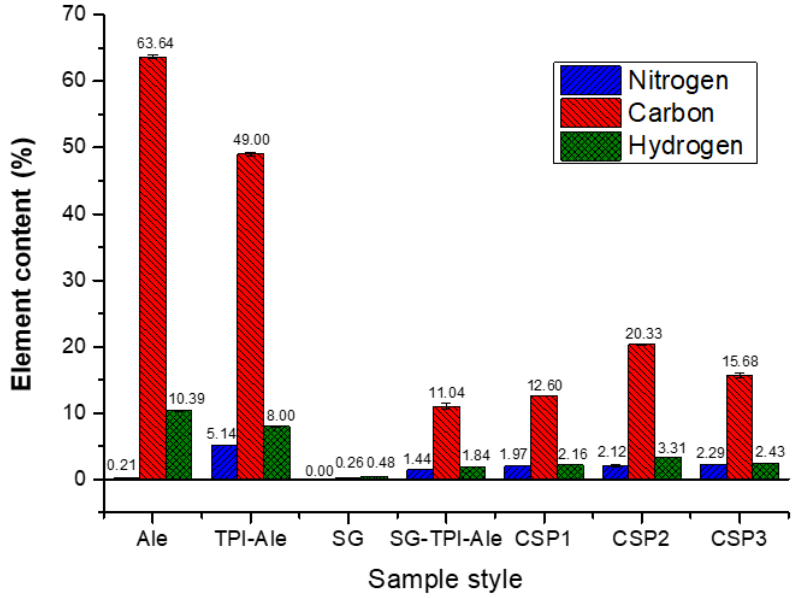

A) Ale, B) TPI-Ale, C) Silica gel, D) SG-TPI-Ale, E) CSP1, F) CSP2, G) CSP3

Fig. 6. Elemental content variation of CSPs for aleuritic acid as chiral arm

Table 1. Heating Loss Ratio of Samples after Aleuritic Acid Was Grafted to Silica Gel

Sample	SG-TPI-Ale	CSP1	CSP2	CSP3
Ration of thermal weight loss/%	17.62	22.31	32.20	25.71
Ration of thermal weight loss of silica gel/%	5.54			
Ratio of net weight loss/%	12.08	16.77	26.66	20.17

From the bonding of TPI-Ale organic molecules on silica gel, CSP1, CSP2, and CSP3 only targeted one functional group and reacted with a substrate with a defined structure, in which both CSP2 and CSP3 reacted with CSP1 terminal carboxyl groups as active sites. It had been shown in the above-mentioned characterization results regarding the structure and grafting ratio that the reaction occurred in preparation process of CSP according to the path in Scheme.1. Then, the products and raw materials in each step had a certain structural formula (assuming that SG-TPI-Ale and CSPs as single bonds were bonded to the surface of silica gel). Therefore, the actual grafting ratio of the reaction at each step can be accurately calculated based on the change in element content in each step.

Table 2. The Calculated Grafting Ratio of CSPs According to Elemental Analysis

Products	SG-TPI-Ale	CSP1	CSP2	CSP3
The structure grafted onto silica gel	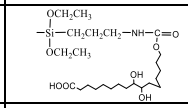	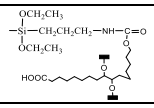	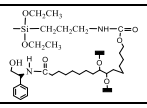	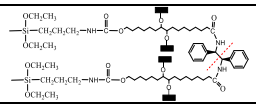
M_F	$C_{24}H_{48}NO_8Si$	$C_{38}H_{52}N_5O_{18}Si$	$C_{46}H_{63}N_6O_{19}Si$	$C_{45}H_{58}N_6O_{18}Si$
M_W	506.8	894.9	1014.1	983.1
C_F	288	456	552	540
C_I	-	168	264	252
C_T	-	12.58	9.88	9.43
C_A	-	1.56	7.73	3.08
G_Y	-	12.40	78.24	32.67

M_F- Molecule formula; M_W- Molecular weight; C_F-Molecular weight of carbon in the structure formula; C_I- The increase of molecular weight of carbon; C_T- Theoretical increase percentage of carbon content; C_A-Actual increase percentage of carbon content; G_Y-Grafting yield

Based on SG-TPI-Ale, the detailed calculation process of the surface modification reaction grafting ratio of the three chiral stationary phase materials is shown in Table 2. The grafting ratio of CSP1, CSP2, and CSP3 was 12.4%, 78.2%, and 32.7%, respectively. For the preparation process of the three stationary phase materials, the order of grafting ratio was CSP2>CSP3>CSP1. The grafting ratio of DNBC to 9,10 site secondary hydroxyl groups of aleuritic acid was the lowest, which may be related to the type of functional groups and steric hindrance of vicinal diol involved in the reaction. The 9,10-site of aleuritic acid was the secondary hydroxyl group, and the esterification reaction was lower than that of the primary hydroxyl group (Heuser *et al.* 2002). In addition, the esterification process of the ortho-dihydroxy group was affected by the double actions of the steric hindrance of the ortho-hydroxyl group and the molecular chain (Watanabe *et al.* 1987). Without considering the difference of different reaction types, CSP2 and CSP3 were amidated at the terminal carboxyl group of the aleuritic acid, and due to small steric hindrance, the reaction was easier to proceed. The grafting ratio of the amidation of the amino compound *S*-PGL using a single chiral center was obviously superior to that of the amino compound *R,R*-DPEDA using double chiral centers, which confirmed the TG test results of CSPs. However, it is important to consider whether the level of grafting ratio determines the quality of the separation effect. Obviously, a separation chromatography test is needed to examine that question.

Separation Test of CSPs Based on Aleuritic Acid as Chiral Spacer Arm

In order to investigate the separation performance of the different structures of aleuritic acid group CSPs, the chiral hydroxyl (compound 1-3), amino (compound 4- 5), chain (compound 1-5), cyclic (compound 7-9), and plane (compound 6) chiral compounds of different structural types were selected in this study (Fig. 7). The separation performance of the aforementioned nine structurally distinct chiral compounds was systematically investigated. The results demonstrated that for stationary phase materials employing aleuritic acid as the chiral spacer arm, enhanced chromatographic resolution was positively correlated with increased configurational complexity of the chiral centers.

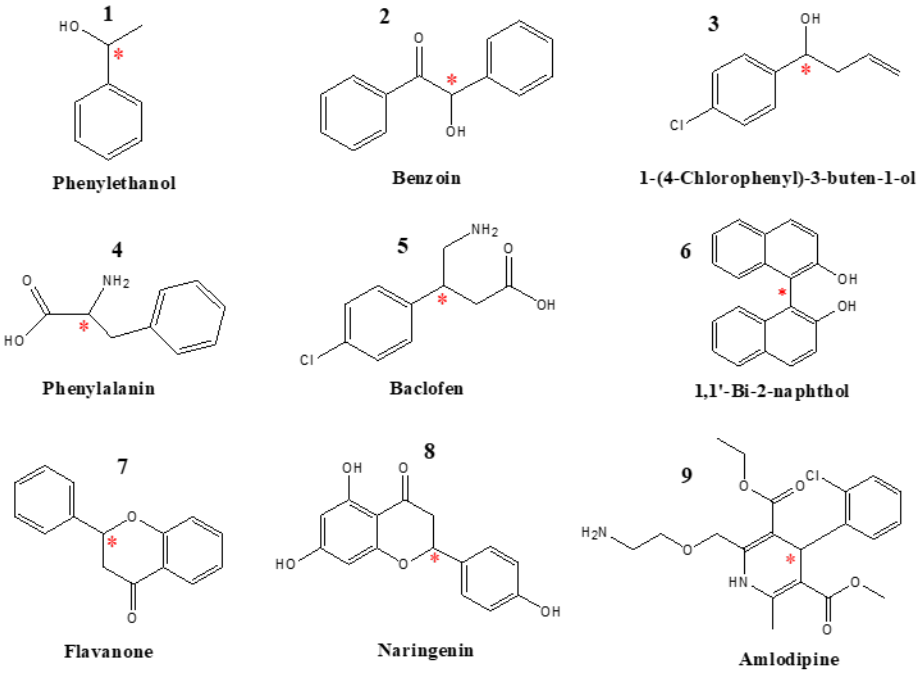

Fig. 7. Compounds enantiomers separated by CSPs of aleuritic acid as chiral arm

Although the grafting ratio of *R,R*-DPEDA in CSP3 was only 32.7%, and the increase of carbon content compared with CSP1 was only 3.1%, which was less than half of CSP2, CSP3 showed significantly higher separation efficiency, and complete separation of 8 chiral compounds had been realized. The introduction of the terminal single chiral center (*S*-phenylglycinol) in CSP2 can facilitate the separation activity to some extent; especially under the condition that the chiral factor had been fixed, it had significant effects on improving the number of theoretical plates and separation effect of the chromatographic column. The formula based on the number of theoretical plates of the chromatographic column was,

$$N = 5.54 \times \left(\frac{t_R}{W_{\frac{h}{2}}}\right)^2 \quad (2)$$

where, N represents the number of theoretical plates of the chromatographic column; t_R is the retention time of the chromatographic peak; and $W_{h/2}$ is the half peak width of the chromatographic peak. Three stationary phase materials (CSP1-3) demonstrating optimal separation efficiency and peak morphology were selected for evaluation. The mobile phase composition was maintained at phenethyl alcohol (Compound 1): methanol: 0.2% ammonium acetate aqueous solution (20:80 v/v). Theoretical plate numbers were

determined through equation (2), yielding values of 4,858, 6,656, and 5,439 plates/m for CSP1, CSP2, and CSP3, respectively. The theoretical plate count followed CSP2 > CSP3 > CSP1. This ranking correlates with chromatographic observations: both CSP2 and CSP3 achieved concurrent chiral separations (Fig. 8), though CSP2 exhibited superior resolution compared to CSP3 (Table 3). The enhanced performance of CSP2 aligns with elemental analysis data showing the highest *S*-PGL grafting ratio. These findings substantiate that when chiral selectivity is structurally predetermined, increased chiral moieties density facilitates compound separation. According to Dalgliesh's "three-point adherence model" (Dalgliesh 1952), in chiral selectors, the more structural types of chiral factors that stationary phase can provide, the easier it was to produce stronger intermolecular forces with the enantiomers of the separated compound, making it easier to achieve chiral separation, which explained why CSP3 had the best separation selectivity. However, due to the grafting ratio of *R, R*-DPEDA in this study, the adaptability of CSP3 to the same compound was not strong enough; although CSP3 showed a stronger separation activity and tendency for the flavanone (compound 7) than the CSP1 and CSP2, effective separation and baseline separation of the three compounds were not achieved.

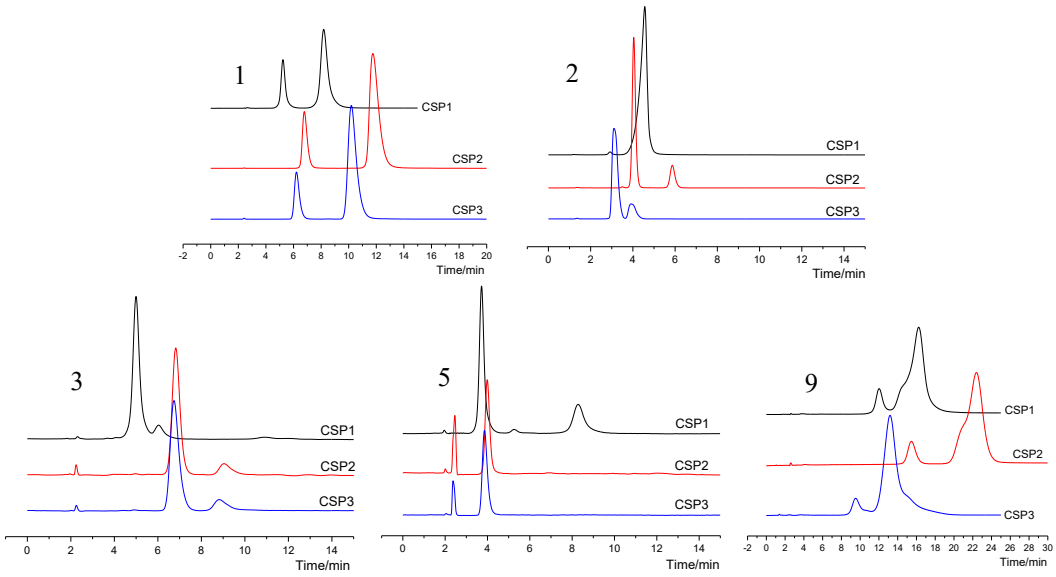

Fig. 8. The chiral separation chromatogram of compounds 1,2,3,5,9 by CSP1-3

Additionally, of note, CSP1 containing only the chiral factor of aleuritic acid still had a higher separation activity, and complete separation of 5 of 9 chiral compounds (compounds 1, 3, 5, 6, 9) was realized. It can be seen that for the chiral stationary phase based on of aleuritic acid as the chiral spacer arm, the spacer arm played the role of a chiral selector due to the presence of 9,10 site chiral hydroxyl groups, indicating that the preparation of stationary phase materials with aleuritic acid as the chiral spacer arm had a good structural basis for chiral separation. And it had further research value and application prospect in the further construction of novel chiral stationary phase materials with chiral spacer arms.

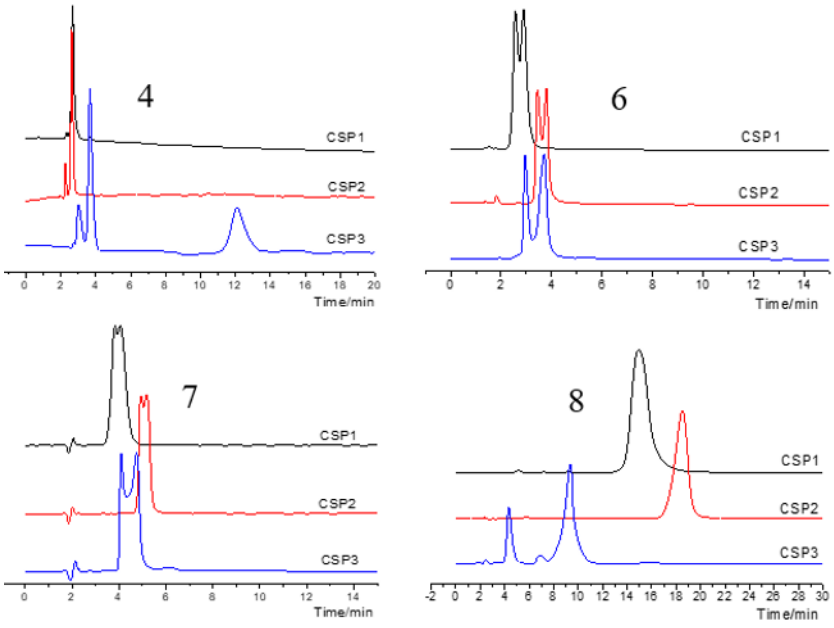

Fig. 9. The chiral separation chromatogram of compounds 4,6,7,8 by CSP1-3

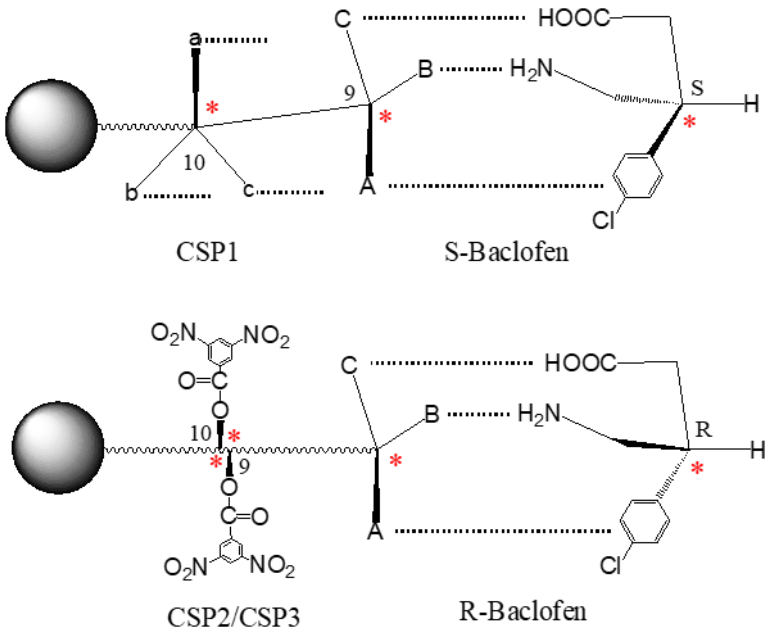

Fig. 10. Three-point interaction model diagram of the peak order for chiral separation of baclofen by aleuritic acid based CSPs

The three CSPs achieved complete separation of eight compounds (Table 3 and Fig. 9), demonstrating that the separation materials employing aleuritic acid as a chiral spacer arm exhibited favorable chromatographic performance. However, it was visually observed from the separation chromatogram that the three CSPs showed significant differences in the separation activity of different chiral compounds. For example, CSP1 could not achieve chiral separation of benzoin (compound 3), phenylalanine (compound 5), and naringenin (compound 8). By contrast, CSP2 not only was about to achieve the separation of benzoin,

but it also had better separation degree than CSP3. For phenylalanine, only CSP3 was able to achieve the separation. For baclofen, although the three CSPs had achieved chiral separation, the order of peaks was completely different, and when separation was conducted by CSP1, the R-configuration first peaked, and then the *S*-configuration peaked. After the chiral factor was derived at the terminus, the separation order of CSP2 and CSP3 was opposite to that of CSP1. This can be understood based on the "three-point interaction model" proposed by Pirkle and associates (Pirkle and Murray 1993; Pirkle and Welch 1992). According to Dalgliesh (1952), the separation of enantiomers was due to the stationary phase and the separated materials being able to form at least three forces. At least one of them was a force with chiral structural characteristic. The formation of a new diastereomeric complex by virtue of the interaction between the stationary phase and the separated compound allowed the separation of the enantiomers only when the difference in retention factor *k* value between the two enantiomers was large enough. If the stationary phase and the R-configuration compound produced an attractive action, then $k_{i,s} < k_{i,R}$, and the S-configuration was eluted first. However, if the stationary phase and the R-configuration compound were repulsive, then $k_{i,s} > k_{i,R}$, and the R-configuration was eluted first. The separation mechanism of CSP1 and CSP2/CSP3 for baclofen can be represented by the three-point interaction model in Fig. 10.

In this study, the origin of the difference in retention factor values is attributed to the spatial location of the chiral factors. CSP1 contains only the 9,10-vicinal diol chiral center in the middle segment of aleuritic acid. This site forms stronger hydrogen bonding or dipole–dipole interactions with S-baclofen, resulting in a stronger retention of the S-enantiomer ($k_{i,s} > k_{i,R}$), and thus the R-baclofen is eluted first. In contrast, CSP2 and CSP3 bear additional aryl amine chiral centers (S-PGL or R,R-DPEDA) at the terminal position. These terminal moieties exhibit superior steric matching and π–π stacking interactions with the R-enantiomer, leading to stronger retention of the R-form ($k_{i,s} < k_{i,R}$), thereby reversing the elution order. For CSP1, given the chiral factor only had the 9,10-site chiral center of aleuritic acid, the 9,10-site chiral center and *S*-baclofen formed a complex by intermolecular forces, so the R-baclofen was eluted first; whereas for CSP2 and CSP3, due to the introduction of the amino-terminal chiral center, the terminal chiral factor had stronger intermolecular interaction with *R*-baclofen, and the *R*-configuration had stronger retention on CSP2 and CSP3, and thus S-baclofen was eluted first. Based on the enantiomeric separation of baclofen, the chiral activity produced in CSP1 was the 9,10-site ortho-dihydroxy of aleuritic acid, while the terminal bonding chiral compound played the role in CSP2 and CSP3. Thus, the mode of action (A, B, C) or the applied force for the different enantiomers of chiral compounds between CSP1 and CSP2 and CSP3 was significantly different.

CONCLUSIONS

Based on aleuritic acid as the chiral spacer arm, the CSP1 containing only aleuritic acid as the chiral factor was successfully prepared by stepwise coupling, and the terminus used *S*-PGL and *1R, 2R*-DPEDA as chiral selectors for CSP2 and CSP3, and the three novel aleuritic acid chiral stationary phases were prepared. The TG, FTIR, EA, and SSNMR characterization of the prepared CSPs showed that the three stationary phases were coupled according to the route design, and the grafting ratio of CSP1, CSP2, and CSP3 was 12.40%, 78.2%, and 32.7%, respectively.

Of the 9 chiral compounds with separation activity, CSP1 achieved successful separation of 4 compounds, accounting for 44.4%; CSP2 successfully achieved separation of 6 compounds, accounting for 66.7%; CSP3 achieved successful separation of 8 compounds, accounting for 88.9%. It can be seen that the CSP with the optical monomer of aleuritic acid as the chiral spacer arm had a certain separation activity, based on which, the introduction of the terminal chiral factor can significantly improve the separation activity; among them, the *R,R*-DPEDA with double chiral centers showed the most significant improvement. The grafting ratio was only 32.7%, and the increase of carbon content compared with CSP1 was only 3.08%, which was less than half that of CSP2, but CSP3 obviously showed higher separation efficiency. The chiral resolution sequence of enantiomers of baclofen was inverse for CSP1 and CSP2/CSP3 due to the difference of chiral factors which determined the interaction of groups between CSPs and enantiomers. This novel chiral stationary phase material based on aleuritic acid as chiral spacer arms has further research value and good application prospects.

ACKNOWLEDGMENTS

This study was financially supported by Natural Science Foundation of Henan [242300420173], Key Research and Development Program of Henan [232102110163], Key Research Planning for Higher Education Institutions in Henan Province [23A550015], Cultivation Foundation Project of Xinyang Agriculture and Forestry University [pyjj20230105], Science and Technology Innovation Team of Xinyang Agriculture and Forestry University (XNKJTD-001).

REFERENCES CITED

Aboul-Enein, H. Y., Kannappan, V., and Kanthiah, S. (2022). "Impact of cyclofructan derivatives as efficient chiral selector in chiral analysis: An overview," *Chirality* 34, 364-373. https://doi.org/10.1002/chir.23396

Ali, M., Hazra, D. K., Kumar, Y. B., and Karmakar, R. (2022). "Improved extraction and recrystallization of high-quality aleuritic acid from natural resins using a modified technique," *Separation Science and Technology* 57, 2916-2922. https://doi.org/10.1080/01496395.2022.2088391

Ali, M., Hazra, D. K., Naiya, H., Sharma, K. K., and Mohanasundaram, A. (2024). "Microwave-assisted extraction and purification of aleuritic acid from seedlac: A fast, eco-friendly and cost-effective single process for enhanced yield and purity," *Chemical Engineering and Processing-Process Intensification* 197, article 109716. https://doi.org/10.1016/j.cep.2024.109716

Ames, D. E., Goodburn, T. G., Jevans, A. W., McGhie J F. (1968). "Synthesis and some reactions of (±)-aleuritic acid," *Journal of the Chemical Society C: Organic* 0, 268-270. https://doi.org/10.1039/J39680000268

Bargmann-Leyder, N., Truffert, J. C., Tambuté, A., and Caude, M. (1994). "Evaluation of Pirkle-type chiral stationary phases by liquid and supercritical fluid chromatography: Influence of the spacer length and the steric hindrance in the vicinity of the stereogenic centre," *Journal of Chromatography A* 666, 27-40. https://doi.org/10.1016/0021-9673(94)80368-4

Benítez, J. J., Guzmán-Puyol, S., Domínguez, E., and Heredia, A. (2015). "Polyester films obtained by noncatalyzed melt-condensation polymerization of aleuritic (9,10,16-trihydroxyhexadecanoic) acid in air," *Journal of Applied Polymer Science* 132, article 41328. https://doi.org/10.1002/app.41328

Benítez, J. J., Heredia-Guerrero, J. A., Cruz-Carrillo, M. A., Morales-Flórez, V., Rosa-Fox, N. D. L., and Heredia, A. (2016). "Biodegradable polyester films from renewable aleuritic acid: Surface modifications induced by melt-polycondensation in air," *Journal of Physics D Applied Physics* 49, article 175601. https://doi.org/10.1088/0022-3727/49/17/175601

Berthod, A., Chang, C.-D., and Armstrong, D. W. (1993). "β-Cyclodextrin chiral stationary phases for liquid chromatography. Effect of the spacer arm on chiral recognition," *Talanta* 40, 1367-1373. https://doi.org/10.1016/0039-9140(93)80212-A

Bui, C. V., Rosenau, T., and Hettegger, H. (2023). "Immobilization of a cellulose carbamate-type chiral selector onto silica gel by alkyne-azide click chemistry for the preparation of chiral stationary chromatography phases," *Cellulose* 30, 915-932. https://doi.org/10.1007/s10570-022-04932-9

Dalgliesh, E. C. (1952). "The optical resolution of aromatic amino-acids on paper chromatograms," *Journal of Chemical Society* 1952, 3940-3942. https://doi.org/10.1039/JR9520003940

Felletti, S., De Luca, C., Mazzoccanti, G., Gasparrini, F., Manetto, S., Franchina, F. A., Chenet, T., Pasti, L., Cavazzini, A., and Catani, M. (2023). "Understanding the transition from high-selective to high-efficient chiral separations by changing the organic modifier with zwitterionic-teicoplanin chiral stationary phase," *Analytical Chemistry* 95, 9630-9637. https://doi.org/10.1021/acs.analchem.3c01344

Francotte, E. R. (2001). "Enantioselective chromatography as a powerful alternative for the preparation of drug enantiomers," *Journal of Chromatography A* 906, 379-397. https://doi.org/10.1016/S0021-9673(00)00951-1

Gonçalves, L., Cravo, S., Fernandes, C., and Tiritan, M. E. (2022). "Development and evaluation of Pirkle-type chiral stationary phase for flash chromatography," *Journal of Chromatography A* 1675, article 463156. https://doi.org/10.1016/j.chroma.2022.463156

Gupta, S., Kashyap, M., Kumar, V., Jain, P., Vinayak, V., and Joshi, K. B. (2018). "Peptide mediated facile fabrication of silver nanoparticles over living diatom surface and its application," *Journal of Molecular Liquids* 249, 600-608. https://doi.org/10.1016/j.molliq.2017.11.086

He, X., Ahmed, A., Guo, S., Kang, C., Shen, Y., Cong, H., and Yu, B. (2022). "Preparation and application of urea-based derivatized β-cyclodextrin chiral stationary phase based on diazotized silica microspheres," *Journal of Chromatography A* 1669, article 462932. https://doi.org/10.1016/j.chroma.2022.462932

Heuser, E., Heath, M., and Shockley, W. H. (2002). "The rate of esterification of primary and secondary hydroxyls of cellulose with p-toluenesulfonyl (tosyl) chloride," *Journal of the American Chemical Society* 72, 670-674. https://doi.org/10.1021/ja01158a007

Ho Hyun, M., and Hun Kim, D. (2004). "Spacer length effect of a chiral stationary phase based on (+)-(18-crown-6)-2,3,11,12-tetracarboxylic acid," *Chirality* 16, 294-301. https://doi.org/10.1002/chir.20038

Lai, X., and Ng, S.-C. (2003). "Mono(6A-N-allylamino-6A-deoxy)perphenylcarbamoylated β-cyclodextrin: Synthesis and application as a chiral stationary phase for HPLC," *Tetrahedron Letters* 44, 2657-2660. https://doi.org/10.1016/S0040-4039(03)00347-2

Li, K., Zhang, W., Liu, L. X., Zheng, H., Li, K., Xu, J., Zhang, H. (2019a). Enantioseparation and thermodynamic properties of aleuritic acid by high performance liquid chromatography with evaporative light-scattering detector (HPLC-ELSD)," *Food Science (Chinese)* 40, 200-207. https://doi.org/10.5555/20193240482

Li, K., Zhang. W., Shi, X. J., Liu, L. X., Li, K., Xu, J., Ma, J. J., and Zhang, H. (2019b). "Preparation of novel mcl-PHA by green synthesis: Influence of active small molecule via esterification effect on side chain," *Materials Research Express* 6, article 075328. https://doi.org/10.1088/2053-1591/ab166c

Li, Y., Shi, G., Kang, S., Zeng, H., Zhang, J., and Wan, X. (2023). "Effect of substituent on the enantioseparation poperty of helical polyacetylene-based chiral stationary phases for high-performance liquid chromatography," *Acta Polymerica Sinica (in Chinese)* 54, 10. https://doi.org/10.11777/j.issn1000-3304.2022.22429

Liu, C., Quan, K., Chen, J., Shi, X., and Qiu, H. (2023). "Chiral metal-organic frameworks and their composites as stationary phases for liquid chromatography chiral separation: A minireview," *Journal of Chromatography A* 1700, article 464032. https://doi.org/10.1016/j.chroma.2023.464032

Ma, Z., Shang, P., Liu, D., Nie, Y., Liu, Y., Guo, X., Wei, B., Bai, L., and Qiao, X. (2023). "Preparation and chromatographic performance of chiral peptide-based stationary phases for enantiomeric separation," *Chirality* 35, 636-644. https://doi.org/10.1002/chir.23564

Nagappayya, S. K., and Gaikar, V. G. (2010). "Extraction of aleuritic acid from seedlac and purification by reactive adsorption on functionalized polymers," *Industrial & Engineering Chemistry Research* 49, 6547-6553. https://doi.org/10.1021/ie902061e

Nawrocki, J. (1997). "The silanol group and its role in liquid chromatography," *J. Chromatogr. A* 779, 29-71. https://doi.org/10.1016/S0021-9673(97)00479-2

Ohji, T., Ohnishi, A., and Ogasawara, M. (2022). "Application of polysaccharide-based chiral high-performance liquid chromatography columns for the separation of regio-, e/z-, and enantio–isomeric mixtures of allylic compounds," *ACS Omega* 7, 5146-5153. https://doi.org/10.1021/acsomega.1c06187

Papp, L. A., Szabó, Z. I., Hancu, G., Farczádi, L., and Mircia, E. (2024). "Comprehensive review on chiral stationary phases in single-column simultaneous chiral–achiral HPLC separation methods," *Molecules* 29(6), article 1346. https://doi.org/10.3390/molecules29061346

Pirkle, W. H., and Murray, P. G. (1993). "Chiral stationary phase design: Use of intercalative effects to enhance enantioselectivity," *Journal of Chromatography A* 641, 11-19. https://doi.org/10.1016/0021-9673(93)83453-Y

Pirkle, W. H., and Welch, C. J. (1992). "Effect of superfluous remote polar functionality on chiral recognition," *Journal of Chromatography A* 589, 45-51. https://doi.org/10.1016/0021-9673(92)80004-E

Qian, H.-L., Xu, S.-T., and Yan, X.-P. (2023). "Recent advances in separation and analysis of chiral compounds," *Analytical Chemistry* 95, 304-318. https://doi.org/10.1021/acs.analchem.2c04371

Scriba, G. K. E. (2012). "Chiral recognition mechanisms in analytical separation sciences," *Chromatographia* 75, 815-838. https://doi.org/10.1007/s10337-012-2261-1

Shi, G., Dai, X., Zhou, Y., Zhang, J., Shen, J., and Wan, X. (2020). "Synthesis and enantioseparation of proline-derived helical polyacetylenes as chiral stationary phases for HPLC," *Polymer Chemistry* 18, 3179-3187. https://doi.org/10.1039/D0PY00205D

Shi, G., Li, Y., Dai, X., Shen, J., and Wan, X. (2022). "Effect of pendant stereostructure on backbone conformation and enantioseparation ability of helical polyacetylene-based chiral stationary phases," *Chirality* 34, 574-586. https://doi.org/10.1002/chir.23414

Sobańska, A. W. (2021). "Emerging or underestimated silica-based stationary phases in liquid chromatography," *Critical Reviews in Analytical Chemistry* 51, 631-655. https://doi.org/10.1080/10408347.2020.1760782

Teixeira, J., Tiritan, M. E., Pinto, M. M. M., and Fernandes, C. (2019). "Chiral stationary phases for liquid chromatography: Recent developments," *Molecules* 24, article 865. https://doi.org/10.3390/molecules24050865

Thunberg, L., Allenmark, S., Friberg, A., Ek, F., and Frejd, T. (2004). "Evaluation of two pairs of chiral stationary phases: Effects from the length of the achiral spacers," *Chirality* 16, 614-624. https://doi.org/10.1002/chir.20080

Wang, X., Li, H., Quan, K., Zhao, L., Qiu, H., and Li, Z. (2021). "Preparation and applications of cellulose-functionalized chiral stationary phases: A review," *Talanta* 225, article 121987. https://doi.org/10.1016/j.talanta.2020.121987

Wang, Z., Wang, W., Luo, A. Q., and Yuan, L.-M. (2024). "Recent progress for chiral stationary phases based on chiral porous materials in high-performance liquid chromatography and gas chromatography separation," *Journal of Separation Science* 47, article 2400073. https://doi.org/10.1002/jssc.202400073

Watanabe, Y., Ogasawara, T., Shiotani, N., and Ozaki, S. (1987). "Stepwise phosphorylation of vicinal diol and sterically hindered alcohol directed toward D-myo-inositol 2,4,5-trisphosphate," *Cheminform* 28, 2607-2610. https://doi.org/10.1016/S0040-4039(00)96160-4

Zhang, J. H., Xie, S. M., and Yuan, L. M. (2022). "Recent progress in the development of chiral stationary phases for high-performance liquid chromatography," *Journal of Separation Science* 45, 51-77. https://doi.org/10.1002/jssc.202100593

Zhang, L., Shen, J., Zuo, W., and Okamoto, Y. (2014). "Synthesis of chitosan 3,6-diphenylcarbamate-2-urea derivatives and their applications as chiral stationary phases for high-performance liquid chromatography," *Journal of Chromatography A* 1365, 86-93. https://doi.org/10.1016/j.chroma.2014.09.002

Zhang, T., Shuang, Y., Zhong, H., Li, L., and Li, L. (2021). "Preparation of a new β-cyclodextrin-bonded chiral stationary phase with thiocarbamated benzamide spacer for HPLC," *Analytical Sciences* 37, 1095-1103. https://doi.org/10.2116/analsci.20P403

Article submitted: May 25, 2025; Peer review completed: June 14, 2025; Revised version received: July 22, 2026; Accepted: July 29, 2026; Published: August 27, 2026.
DOI: 10.15376/biores.21.4.10108-10126